Neuroscience 121 (2003) 141–154

THE HUMAN PRIMARY SOMATOSENSORY CORTEX RESPONSE CONTAINS COMPONENTS RELATED TO STIMULUS FREQUENCY AND PERCEPTION IN A FREQUENCY DISCRIMINATION TASK

L. C. LIU,* P. B. C. FENWICK, N. A. LASKARIS, M. SCHELLENS, V. POGHOSYAN, T. SHIBATA AND A. A. IOANNIDES

Laboratory for Human Brain Dynamics, RIKEN Brain Science Institute, 2-1 Hirosawa, Wako-shi, Saitama, 351-0198, Japan

Abstract—Somatosensory stimulation of primary somatosensory cortex (SI) using frequency discrimination offers a direct, well-defined and accessible way of studying cortical decisions at the locus of early input processing. Animal studies have identified and classified the neuronal responses in SI but they have not yet resolved whether during prolonged stimulation the collective SI response just passively reflects the input or actively participates in the comparison and decision processes. This question was investigated using tomographic analysis of single trial magnetoencephalographic data. Four right-handed males participated in a frequency discrimination task to detect changes in the frequency of an electrical stimulus applied to the right-hand digits 2+3+4. The subjects received approximately 600 pairs of stimuli with Stim1 always at 21 Hz, while Stim2 was either 21 Hz (50%) or varied from 22 to 29 Hz in steps of 1 Hz. Both stimuli were 1 s duration, separated by a 1 s interval of no stimulation. The left-SI was the most consistently activated area and showed the first activation peak at 35–48 ms after Stim1 onset and sustained activity during both stimulus periods. During the Stim2 period, we found that the left-SI activation started to differ significantly between two groups of trials (21 versus 26–29 Hz) within the first 100 ms and this difference was sustained and enhanced thereafter (approximately 600 ms). When only correct responses from the above two groups were used, the difference was even higher at later latencies (approximately 650 ms). For one subject who had enough trials of same perception to different input frequencies, e.g. responded 21 Hz to Stim2 at 21 Hz (correct) and 26–29 Hz (error), we found the sustained difference only before 650 ms. Our results suggest that SI is involved with the analysis of an input frequency and related to perception and decision at different latencies.

Key words: MEG, primary somatosensory cortex, electrical stimulation, single trial analysis, steady-state responses, perception.

Both animal and human studies have provided direct evidence that somatosensory cortical areas are highly and rapidly adaptive (Braun et al., 2000; Romo and Salinas, 2001). Recent animal studies by the Romo group (Hernandez et al., 2000; Salinas et al., 2000), in which they trained monkeys to discriminate between the frequencies of two flutter stimuli presented sequentially on a fingertip, showed that neurons in the primary somatosensory cortex (SI) generated a neural representation of vibrotactile stimuli that correlated closely with performance. Further, discrimination based on microstimulation injected into SI neurons is indistinguishable from that produced by natural stimuli (Romo et al., 1998, 2000). These findings thus established a strong link between the neuronal activity of SI and the sensory component of the discrimination task. The authors suggested that this sensory activity provided input into memory and decision-making mechanisms distributed over a wide cortical network (Romo and Salinas, 2001). Studies about how decisions are made increasingly place the emphasis on the prefrontal cortex (Schall, 2001; Miller and Cohen, 2001; Hernandez et al., 2002), but there are still unresolved questions about the role of the SI area concerning decision making after the initial processing of the input. For humans it is difficult to study the SI contribution to early perception and decision-making because the methods used for animal experiments are not applicable in human studies.

To investigate non-invasively whether the human SI possesses similar properties to those reported in monkeys, we gave four right-handed male subjects a frequency discrimination task in which they had to distinguish between and estimate the frequency of a "comparison" stimulus (Stim2) after a "standard" stimulus (Stim1) had been given to the right-hand digits 2+3+4. Each subject received approximately 600 pairs of stimuli. Stim1 and Stim2 were 1 s duration and delivered consecutively, separated by a fixed inter-stimulus delay of 1 s. At the end of Stim2, the subjects responded verbally with an estimate of the Stim2 frequency rather than using a same–different discrimination. One hundred eighty trials of magnetoencephalographic (MEG) signals were recorded using a whole-head system. Tomographic localization of activity throughout the brain was computed from 500 ms before the onset of Stim1 to 500 ms after the offset of Stim2 (total duration of 4 s) for 60 selected single trials. The finger area of the left-SI was functionally identified and the time course of its activity was then extracted and correlated with the subjects' responses on a single trial basis. Our study follows in spirit the very successful series animal studies by the Romo group. By

*Corresponding author. Tel: +81-48-467-7218; fax: +81-48-467-9731.
E-mail address: lichan@brain.riken.go.jp (L. C. Liu).

Abbreviations: ICA, independent component analysis; MDS, multidimensional scaling; MEG, magnetoencephalography; MFT, magnetic field tomography; MPC, medial premotor cortex; MST, minimal spanning tree; ROI, region of interest; RQ, Rayleigh Quotient; SI, primary somatosensory cortex; SII, secondary somatosensory cortex; SNR, signal to noise ratio; VPM, ventral posterior medial.

0306-4522/03$30.00+0.00
doi:10.1016/S0306-4522(03)00353-1

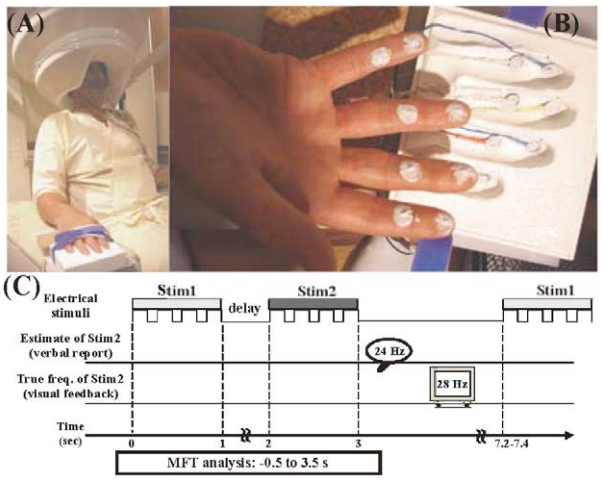

Fig. 1. (A, B) Experimental setup. (C) Schematic diagram of the frequency discrimination task.

asking the subjects to estimate the input frequency, we have introduced a change in the paradigm to exploit the human's language ability. This refinement allowed us to use robust statistical analysis to study the SI responses over a relatively small number of trials available while the subjects' performance was improving but before they had mastered the task.

EXPERIMENTAL PROCEDURES

Subjects and experimental setups

Four healthy drug free right-handed male subjects (1–4; 39±13.2 years) volunteered for the MEG experiment. Informed consent was obtained in accordance with the Declaration of Helsinki and the study was approved by the RIKEN ethical committee. For each subject, a plaster hand mold free of magnetic contamination was made to achieve a reliably fixed hand position and so ensure stimulation of the same skin sites (Fig. 1A). An elastic strip was also used to maintain contact of the fingers with the hand mold. Pairs of stimulating electrodes were placed on the palmer surface of the distal and middle segments of digits 2, 3 and 4 (Fig. 1B). A Grass stimulator (model S8800; Astro-Med Inc., West Warwick, RI, USA) controlled the electrical stimulation (0.2–2.9 mA, trains of 0.3 ms square wave pulses). Before the experiment, a threshold setting of the strength of the 21 Hz stimulus was carried out for each finger so as to achieve a detectable, reliable, comfortable and comparable buzzing sensation across the digits. The intensity of the stimulation was adjusted individually for each digit of each subject and thereafter fixed for the whole experiment.

The discrimination task (Fig. 1C) was completed in about 4 h. In summary, the subjects had to detect small changes in frequency by estimating the frequency of the second stimulus (Stim2) after the first stimulus (Stim1) had been presented to the right-hand digits 2+3+4. Stim1 and Stim2 were 1 s duration. The two stimuli were delivered consecutively, separated by an inter-stimulus delay of 1 s. Stim1 was always 21 Hz, while Stim2 was either 21 Hz (50%) or a frequency randomly selected from 22 to 29 Hz (6.25% for each frequency). At the end of Stim2, the subjects reported verbally the estimated frequency of Stim2. A visual feedback of the correct frequency of Stim2 (visual angle approximately 4°) was displayed at the center of a screen approximately 56 cm in front of the subjects 2.5 s after the offset of Stim2. Inter trial intervals were randomized in duration between 1.4 and 1.6 s with a mean of 1.5 s. Subject 1 received 380 trials of Stim1-Stim2, which was divided into two blocks and each block contained 19 runs (10 trials of Stim1-Stim2 in each run). Both the behavior and MEG data were recorded in each run. For subjects 2–4, taking into account that the MEG recording during a run required additional time for head localization (at the beginning and end of the run) and for data transfer, we therefore recorded the MEG signals once every three runs to limit the subject's time inside the shielded room and the duration of the experiment. Subjects 2–4 received 576 trials, divided into three blocks, each contained 13 runs (approximately 15 trials per run, lasting roughly 3 min). The subjects' behavioral data were collected for all the runs.

MEG signal recording and processing

We recorded MEG signals using the whole head Omega 151-channel system (CTF Systems Inc., Vancouver, BC, Canada) with additional electrodes to monitor the subjects' artifacts from vertical eye movement (EOG electrodes 1 cm above and below the left eye), horizontal eye movement (EOG electrodes 1 cm lateral to the left and right outer canthus of the eyes), heart function (ECG electrodes, left and right wrists, left and right ankles and lead V2) and the subjects' speech-related myographic activity (EMG electrodes, left and right cheeks). The MEG signal was recorded, after low-pass filtering at 150 Hz and sampling at 625 Hz, in a continuous mode for each run (approximately 3 min). Off-line the environmental noise was first removed from the MEG signal by forming the third gradient of the magnetic field and the resulting data were filtered in the 1.25–150 Hz band using the CTF software. The subjects' artifacts were removed using independent component analysis (ICA; Jahn et al., 1999). Processed MEG single trial signals were then extracted from the ICA-cleaned MEG signal from 500 ms before the onset of Stim1 to 500 ms after the offset of Stim2 (total duration of 4 s) for each recorded comparison pairs of Stim1-Stim2.

Before the MEG experiment three head coils were attached to the subject's scalp (nasion, left and right pre-auricular points). The three coils defined a coil-based coordinate system. The subject's head shape was scanned using a 3D digitizer (Polhemus, Colchester, VT, USA). The digitized head shape was fitted to the subject's MRI to obtain a transformation matrix between the coil- and MRI-based coordinate systems using in-house software. The results for the co-registration were checked manually, and if the fit was not accurate the digitization process was repeated. In each recording run, the subject's head position was monitored with the three head coils before and after each MEG recording run.

Performance for frequency discrimination

We evaluated each subject's performance in two ways. For Stim2=21 Hz (i.e. same frequency as Stim1), we calculated the percentage of correct trials (%correct), i.e. input Stim2=21 Hz, response=21 Hz. To maintain the consistency of the psychophysical measure used in earlier "same–different" paradigms (Recanzone et al., 1992; Liu et al., 2000), at each Stim2>21 Hz (i.e. 22–29 Hz, different frequency from Stim1), we calculated a performance score P with $P=P(H)\times[1-P(FA)]$, where P(H) and P(FA) were the probability of a hit and a false alarm, respectively. Based on the input frequencies of Stim2 and the subject's responses, we classified all trials as hits, misses, false alarms and correct rejections (hits: input Stim2>21 Hz and response>21 Hz; misses: input Stim2>21 Hz and response=21 Hz; false alarms: input Stim2=21 Hz and response>21 Hz; correct rejections: input Stim2=21 Hz and response=21 Hz). Hence for each Stim2 frequency (i.e. 22–29 Hz), the probability of a hit was calculated as P(H)=(no. hits)/(no. stimulus presentations), while the probability of a false alarm P(FA)=(no. false alarms)/(no. stimulus presenta-

tions). The performance score P indicates how well the subject could distinguish Stim2 from Stim1. P goes to 1 if the subject responded "different" (i.e. not 21 Hz) when Stim2>21 Hz and responded "same" (i.e. 21 Hz) when Stim2=21 Hz.

Magnetic field tomography analysis

Magnetic field tomography (MFT) produced probabilistic estimates for the non-silent primary current density vector $\mathbf{J}(\mathbf{r}, t)$ at each time slice of the MEG signals (Ioannides et al., 1990). For each computation the sensor locations were expressed in the MRI coordinates of the subject so that each single trial was computed in the same source space which covered the whole brain. Because the MEG signal was recorded separately for each run (each run contained 15 pairs of Stim1-Stim2) and the subjects were allowed to move between runs, the MEG signals could not be analyzed by averaging the data with respect to the stimulus onset. Moreover, we aimed to correlate the subjects' brain responses with their performance data and hence our overall analysis was carried out on a single trial basis. However, the full MFT computation for all MEG single trial signals results in too many 3-D images to inspect individually. For each subject, we therefore applied MFT to extract estimates of brain activity from 60 of the recorded 180 MEG single trial signals. Trials with small head movement in the runs (<3 mm) were specially selected and covered the frequency ranges of Stim2 (21–29 Hz) and the subjects' responses (correct and incorrect with 1–8 Hz error). They were drawn as evenly as possible from the three training blocks. The selected single trials therefore consisted of approximately 24 trials of Stim2 at 21 Hz (slightly different numbers across the subjects) and the remainder (approximately 36) trials of Stim2 at 22–29 Hz based either on Stim2 frequency, or approximately 20 correct and approximately 40 incorrect trials determined from the subjects' responses.

MFT was applied to each MEG single trial signal separately in steps of 3.2 ms and so produced a sequence of probabilistic estimates for the instantaneous current density $\mathbf{J}(\mathbf{r}, t)$ in the interval from −500 to 3500 ms relative to the onset of Stim1 (i.e. 1250 time slices). For each of the 60 trials from each subject, MFT analysis produced the 3D distribution of activity throughout the source space at each time slice. Since each single trial MFT solution is computed in the same source space (co-registered with the subjects MRI) it is feasible to arrange the 60 MFT solutions time slice by time slice. The result is the instantaneous average distribution for each time slice, capturing the time locked components of the activation. By inspecting the averaged current density vector field smoothed with a moving window of 25.6 ms in steps of 12.8 ms, strongly and consistently activated areas in the region of SI were identified. A region of interest (ROI) was then defined as a sphere centered at the identified focus with a radius of 1.0 cm and labeled by its anatomical position. We discuss the results of the analysis of the ROI sampling activity from the left-SI. It should be noted that the average MFT solution was only used for determining the location of the ROI. All the analyses were carried out on the unaveraged data and on a trial-by-trial basis. The single trial (i) activation curve (acv-curve, $x_i(t)$) for the left-SI ROI, $x_i(t)=J^i_1(t)$, was calculated along the main direction of the current density as a function of time, where $J^i_1(t)=\int_{ROI}\mathbf{J}(\mathbf{r}, t)\cdot\hat{\mathbf{u}}_{ROI}d^3\mathbf{r}$ with $\hat{\mathbf{u}}_{ROI}$ defined as the direction of the current density vector at the maximum (modulus) of the MFT activation. The acv-curves $x_i(t)$, t=1:1250, i=1:60 were treated as temporal patterns. Pattern recognition principles were utilized to determine the encoding and information processing scheme employed in the left-SI ROI during the learning of the frequency discrimination task.

Pattern analysis of single trial activation curves

Grouping of single trials. Each single trial acv-curve was labeled according to the input frequency of Stim2 and the subjects' response. This labeling enabled a classification either by a single or by both labels, thus allowing for testing response similarity within/across the resulting groups. For example, using the first label the left-SI responses were grouped into 21 and 26–29 Hz (input frequency of Stim2), while using the second label they were grouped into correct and incorrect responses. It was not possible to form some groups for some subjects (e.g. for subject 4, forming a group of correct responses to the 26–29 Hz of Stim2) because there were not enough single trials available. The single trial acv-curves were used to perform within group analysis and validation using signal-to-noise ratio (SNR) measurements. In addition they were used to perform time-dependent comparisons between groups using a discriminative analysis of patterns that was essentially similar to the one previously employed to contrast spatial patterns of brain activity in response to conditioned stimuli (Barrie et al., 1999).

SNR measurements. To quantify the signal content in the ensemble of single trial acv-curves, a conventional SNR estimator (Raz et al., 1988) was used with a moving window. At each time slice t, a segment $X_i(t, p)=\left[x_i\left(t-\frac{p-1}{2}\right), \ldots, x_i(t-1), x_i(t), x_i(t+1), \ldots, x_i\left(t+\frac{p-1}{2}\right)\right]$ consisting of p=31 samples (i.e. approximately 100 ms) was extracted from each single trial acv-curve and used in the computation of noise power (NP) and signal power (SP) using the following equations (Laskaris et al., 1997):

$$\bar{X}=\frac{\sum_{i=1}^{N}X_i(t, p)}{N},\ NP=\frac{\sum_{i=1}^{N}\|\bar{X}-X_i(t, p)\|^2_{L_2}}{p(N-1)},\ SP=\frac{1}{p}\|\bar{X}\|^2_{L_2}-\frac{1}{N}NP,$$

$$\mathrm{SNR}=\frac{SP}{NP}$$

The SNR measurement is sensitive to both transient time-locked and phase-reorganization events, provided they emerge coherently across the set of single trial acv-curves. Therefore, the resulting time-dependent curve SNR(t) peaks at the latencies where the set of acv-curves are most similar. In addition, the SNR measurement was used to identify the possible significant role that the different frequency bands could play in stimulus encoding and processing. To this end, the single trial acv-curves were filtered in a zero-phase distortion mode within three well-defined frequency bands, namely, 8–15 Hz, 18–30 Hz and 35–80 Hz, using the finite impulse response filters with the filter order of 50 available in the commercial software package IDL (Research Systems Inc., Boulder, CO, USA). The SNR measurements were repeated for these filtered acv-curves and compared with the ones filtered in wide band (1.25–150 Hz).

Discriminative analysis of single trials

Groups of single trial acv-curves were contrasted in pairs using the Rayleigh Quotient (RQ), an index that is often employed in feature selection prior to the construction of a classifier (Cohen, 1986). A window of 100 ms (p=31 samples) scanned concurrently the two groups of acv-curves $x_i(t)$ and $y_j(t)$ (i=1:N_x, j=1:N_y). At each time slice t, the corresponding groups of segments $X_i(t, p)$ and $Y_j(t, p)$ were used in the RQ index computation:

$$RQ(t)=\frac{\|\bar{X}-\bar{Y}\|^2_{L_2}}{Var_x+Var_y} \quad (1)$$

$$\bar{X}=\frac{\sum_{i=1}^{N_x}X_i(t, p)}{N_x},\ \bar{Y}=\frac{\sum_{j=1}^{N_y}Y_j(t, p)}{N_y},\ Var_x=\frac{\sum_{i=1}^{N_x}\|\bar{X}-X_i(t, p)\|^2_{L_2}}{N_x-1},$$

$$Var_y=\frac{\sum_{j=1}^{N_y}\|\bar{Y}-Y_j(t, p)\|^2_{L_2}}{N_y-1}$$

The RQ(t)-curve provides a time-dependent quantification of the separability between the two groups of acv-curves and it can be

regarded as an SNR-index quantifying coarsely the clustering tendency of the two groups being analyzed. High RQ values emerge naturally at the latencies where the given grouping corresponded to morphological differences between the analyzed groups. The flexible character of the RQ index and its independence on the number of single trials included in each group enabled us to compare different partitions of the single trial acv-curves and also to study the effect of different representations for the single trial acv-curves on the obtained grouping-validity. For the latter case, the single trial acv-curves were filtered in the above three frequency bands and the RQ index for a given grouping of trials was compared across the three filter bands and also contrasted with the corresponding RQ from the wide-band analysis.

To provide an indication of the significance of the RQ indices, a randomization test was employed (Jain and Dubes, 1988). The acv-curves which participated in the whole set under test were split randomly into two sub-sets (groups) having N_x and N_y number of acv-curves and the RQ(t) were recalculated. The empirical distribution formed for each time slice t separately, from 100 repetitions of this procedure was used to draw the 95% confidence level (significant $P<0.05$) corresponding to the "null hypothesis" that the overall set of the (N_x+N_y) acv-curves had been split randomly.

MULTIDIMENSIONAL SCALING (MDS)

A dimensionality reduction technique of distance preserving character (a form of cluster analysis), known as classic MDS, was utilized as a means of (i) improving the RQ-based discriminative analysis, (ii) enabling the visualization of the data structure and (iii) providing a further interface for exploratory data analysis.

(i) In short, two groups of acv-curve segments $X_i(t, p)$ and $Y_j(t, p)$ were considered as points in a p-dimensional space so that the inter-point distances reflected the corresponding morphological differences between the segments. MDS provided a two-dimensional image of the overall point set that was found to make the discriminative analysis more robust (Barrie et al., 1999; Laskaris and Ioannides, 2002). For this reason, in this paper the segments in all the RQ computations (Eq. 1) have been replaced by their MDS-based images.

(ii) At the significant peaks of the RQ(t) curve, MDS allowed a detailed look at the distribution of members of the two sets (with N_x and N_y acv-curve activations) in the overall topology. Since a high RQ value was a sufficient condition for the clear separation between the two groups, acv-curve segments were extracted for latencies around the peak in the RQ(t) curve, analyzed and plotted as two-dimensional points on an MDS map.

(iii) The computed map was then incorporated in a guided user interface environment (Laskaris and Ioannides, 2001) that facilitated the study of the signal characteristics responsible for the calculated structure. Specifically, the graphical representation of the emerged structure, via the minimal spanning tree (MST), enabled the extraction of typical responses summarizing the left-SI ROI activation for each group of acv-curves.

RESULTS

Behavioral results

All four subjects were able to cooperate with the experimental situation and coped easily with the 4 hours in the magnetometer. The subjects' hands were placed comfortably in the mold, ensuring that the same electrode positions were used for the entire experimental period and stimulation of the fingers was successfully carried out. All four subjects reported that the task was challenging because the difference in the buzzing sensation induced by the electrical stimulation at different frequencies was subtle. Although Stim1 was always at 21 Hz, the subjects found it necessary to attend to Stim1 to judge Stim2 correctly. Fig. 2(A) shows the performance of each subject in each block in terms of %correct for Stim2 at 21 Hz: all four subjects had better performance in blocks 2 and 3 compared with block 1 and performed best in block 2, which indicates some learning during the second block. However, the subjects then plateaued in their learning and no further improvement was seen during the third block, which was likely due to subjects' fatigue toward the end of the 4-h experiment. Fig. 2 (B) and (C) show the performance score P for each Stim2 different from Stim1 (22–29 Hz). Fig. 2 (B) is the P values for each subject averaged over the three training blocks (subject 1: two blocks): subject 1 performed best while subject 4 was the worst. Although subject 4 had improved his performance for the "same" trials (Stim2=21 Hz as shown in Fig. 2A), he could not entirely distinguish the "different" trials (Stim2=22–29 Hz) and his performance was below chance ($P=0.5$). Excluding subject 4, averaged over subjects 1–3, the P values for each training block are shown in Fig. 2 (C): subjects 1–3 improved their performance for Stim2 at 26–29 Hz in blocks 2 and 3, with the best performance in block 2 among the three blocks. The subjects found the discrimination for Stim2 at 22–25 Hz to be difficult: they improved the performance in block 2 compared with block 1, but not in block 3. For Stim2=22 Hz, the closest frequency as Stim1 and hence most difficult to discriminate from Stim1, the improvement was not evident. To discriminate closely matched Stim2 frequencies from Stim1, the subjects would need longer than 4 h for the discrimination training. Before the subjects master the discrimination, the performance would depend more on the subjects' effort on determining the Stim2 frequencies and hence would be more affected by subjects' fatigue such as in block 3 than in block 1. Averaged over the three blocks from subjects 1–3, the threshold to detect a frequency difference relative to 21 Hz on 50% of the trials ($P=0.5$) was about 5 Hz (i.e. Stim2≥26 Hz).

MEG results

For all four subjects the most consistently activated area was over the left-SI in the region of the hand area. This area, together with its Talairach coordinates for all four subjects, is shown in Fig. 3. Both the location and current direction of the left-SI ROI are shown and defined by examining the averaged MFT solutions (not shown but used only for ROI definition), which had the first major activation in the left-SI ROI after the onset of Stim1, for subjects 1 and 2 at 48.0 ms, subjects 3 and 4 at 35.2 ms.

The single trial acv-curves for the left-SI ROI were computed and the comparison of the SNR-measurements

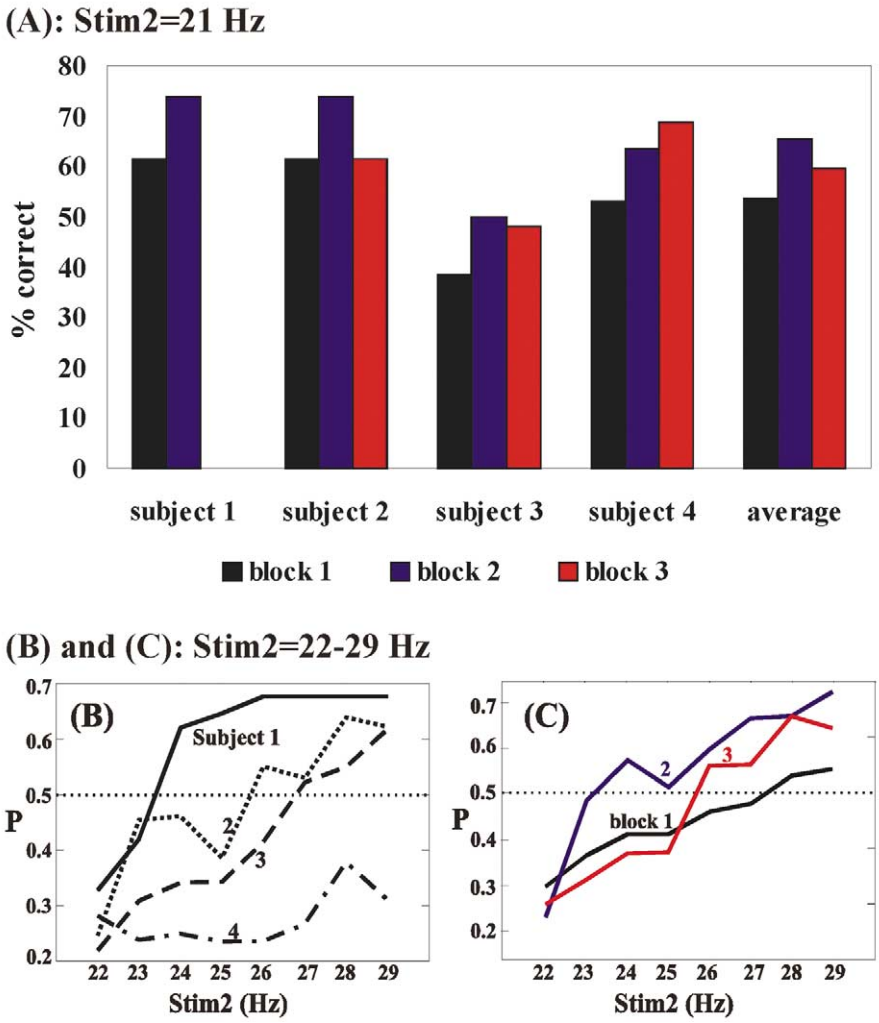

Fig. 2. Behavioral performance: (A) %correct for Stim2=21 Hz and (B, C) performance score P for Stim2=22–29 Hz. (A) %correct was shown for each subject in each block, with the average over all four subjects in the most right column. (B) The performance score P averaged over the training blocks for each subject (shown in different line styles). (C) The P values averaged over subjects 1–3 for each block (shown in different colors). The thin horizontal lines indicate the chance level of discrimination at 50% in (B) and (C).

from the four different frequency bands showed that, for all four subjects, the 18–30 Hz frequency band contained the most information regarding Stim1 and Stim2, although the signal power was higher in the 8–15 Hz than the 18–30 Hz and 35–80 Hz. It was found that the inclusion of other frequency bands in the wide-band signal reduced the SNR. The importance of the 18–30 Hz frequency band was further confirmed by the discriminative analysis. The RQ values from the filtered acv-curves at 18–30 Hz were higher for the grouping we studied than those from the other three frequency bands. For this reason, in the following presentation, we will restrict ourselves only to the results from the analysis of the acv-curves filtered in the 18–30 Hz frequency band.

For each subject the filtered acv-curves and the corresponding averages (used for display only) for both Stim1 and Stim2 at 21 Hz are shown in the right hand column of Fig. 3. For all four subjects rhythmic driving of the left-SI area is clearly apparent during Stim1 and Stim2. The corresponding SNR(t) computed from the filtered 21–27 acv-curves is shown in the bottom row below the average trace. High SNR values are seen for each subject during almost the whole Stim1 and Stim2 period. The high SNR values in the Stim1 and Stim2 period suggest that information reaches the left-SI in the 18–30 Hz frequency band and that the area processes information during the stimulation periods.

To investigate the way this information is handled by left-SI we used the RQ analysis to compare the signal characteristics between Stim1 and Stim2. As mentioned the RQ(t) provides a time-dependent quantification of the separability between the two groups of acv-curves and it can be regarded as an SNR-index quantifying coarsely the clustering tendency of the groups being analyzed. High RQ values are found at the latencies where there are morphological differences between the analyzed groups. We predicted that the Stim2 period would not be similar when compared with the Stim1 period across its entire time range and that it would

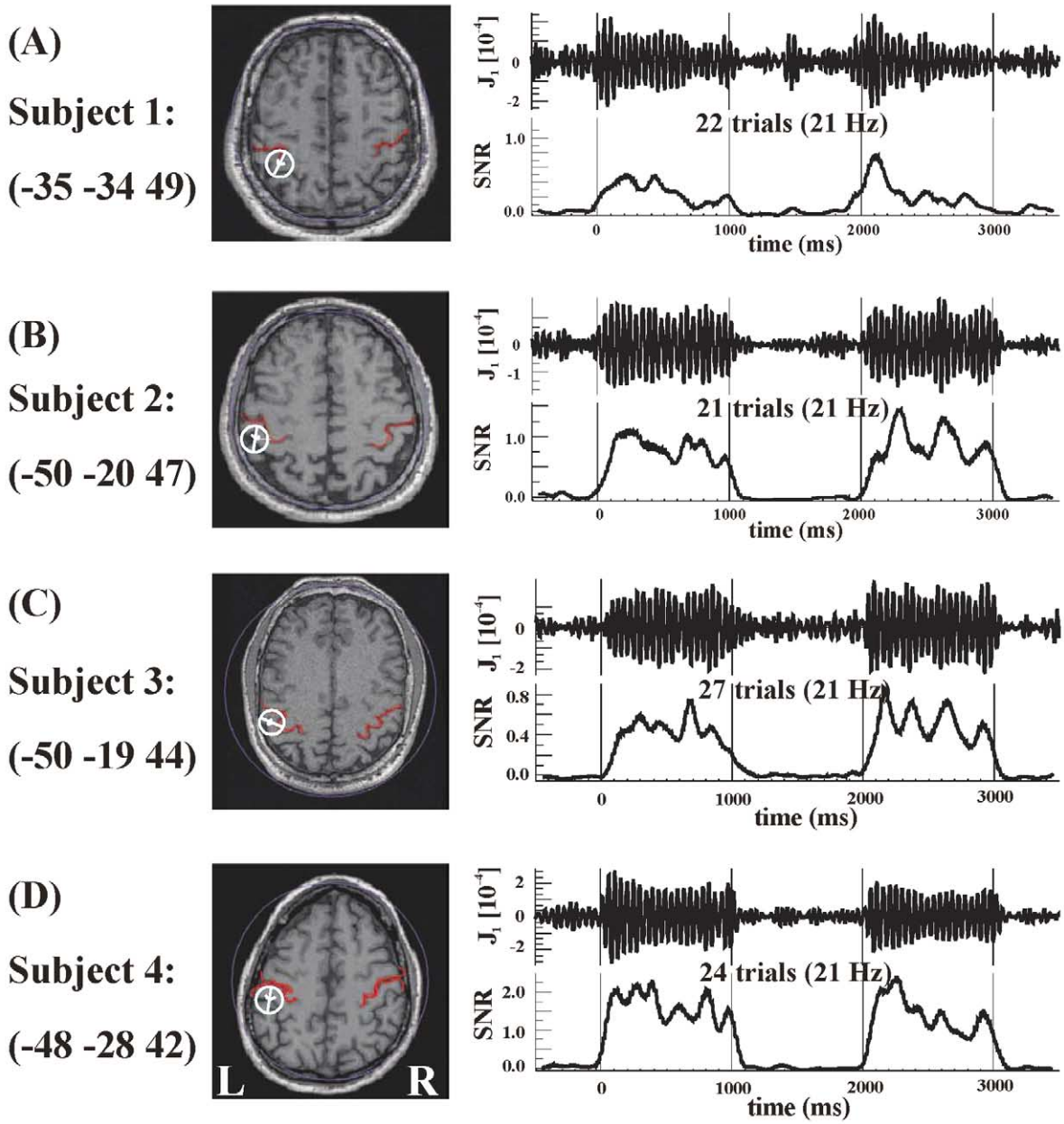

Fig. 3. Subjects 1–4 (A–D): left column, ROI definition for the left-SI area characterized by the average MFT curves of the set of 60 processed MEG single trials for each of the four subjects. The ROI is plotted as a small white circle with a white arrow indicating the main direction of the current density vector, superimposed onto each subject's axial MRI slice with the central sulcus highlighted in red. The Talairach coordinates are printed for reference on the left of each MRI. Right column, the top row is the average trace (for display only) of the 18–30 Hz filtered (approximately 24) acv-curves for Stim2 at 21 Hz. In the bottom row below the average trace is the corresponding SNR(t)-curve computed from the acv-curves.

show components related to signal frequency recognition and to making a decision about the same or different comparison of Stim2. To test this we used the trials of Stim2 at 21 Hz only and computed the RQ between Stim1 period (−450–1450 ms) and Stim2 period (1550–3450 ms).

Fig. 4 shows the results, for each of the four subjects, the thick black line shows the RQ level for the comparison, while the thin lines on either side of the RQ curve mark the $P<0.05$ significance levels. Subjects 1–3 show non-significant changes for the first 150 ms then for subjects 2–4 the change is significant until about 500–600 ms and then rises again significantly towards the end of the trial, although this rise is less marked than that at the beginning. This raises the question as to whether the early part of the Stim2 period is related to analyzing the second frequency (Stim2) while the end of the period could be related to a perception and decision.

To test the first of these two hypotheses we contrasted the 26–29 Hz trials of Stim2 against the 21 Hz of Stim2. We predicted an early rise in RQ(t) after the onset of Stim2 as the second frequency was novel (not 21 HZ), and that there would be increasing characterization of the Stim2 frequency as the Stim2 epoch progressed.

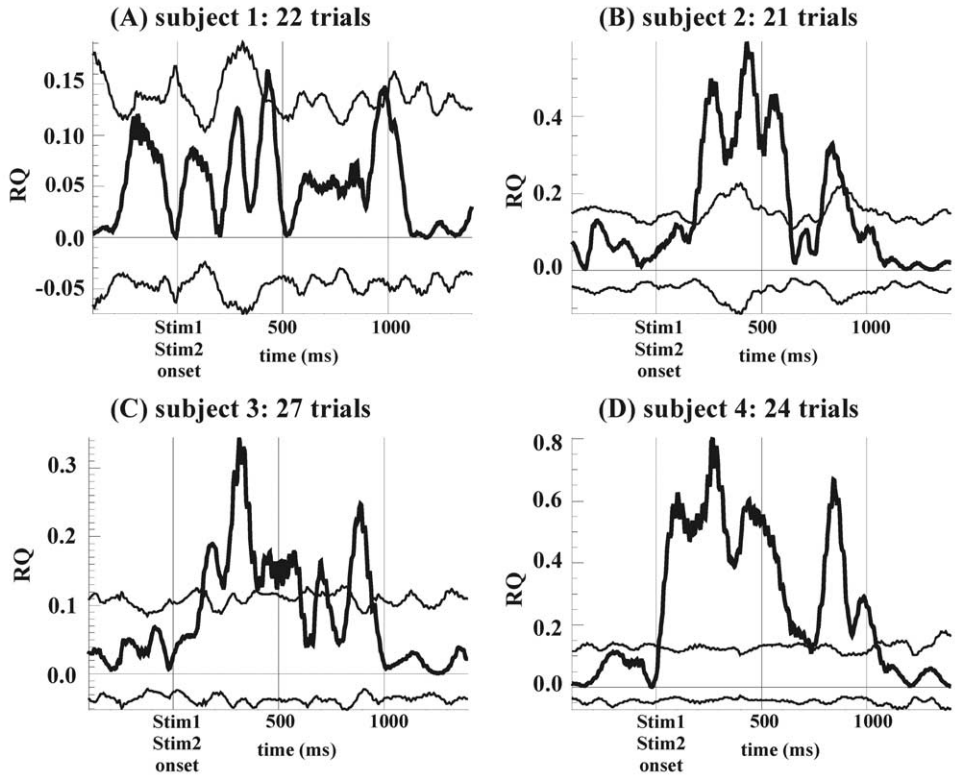

Fig. 4. Subjects 1–4 (A–D): RQ(t) curve for comparison between the 21 Hz Stim1 (−450–1450 ms relative to Stim1 onset) and 21 Hz Stim2 (1550–3450 ms relative to Stim1 onset or −450–1450 ms relative to Stim2 onset). The thick black line shows the RQ level while the two thin lines on either side of the RQ curve mark the $P<0.05$ significance level. The number of trials used for the RQ computation is also printed above the curves for reference.

Fig. 5 shows the RQ(t) obtained from the Stim2 at 21 Hz versus 26–29 Hz with the number of trials given above the RQ(t) in the left column: the thick black line shows the RQ(t), while the thin lines on either side of the RQ(t) mark the $P<0.05$ significance levels. For all four subjects the RQ(t) becomes significant for the first time soon after the Stim2 onset (50–100 ms), then remains significant for the rest of the trial for subjects 2–4 and intermittently for subject 1. To examine differentiation as the epoch progressed we applied the MDS analysis to the acv-curve segments extracted for latencies around the two early significant peaks of the RQ(t)-curve, marked with a brown (early) and green (later) bar. The resulting two-dimensional MDS maps are shown in middle and right columns of Fig. 5. Above the MDS maps are the time ranges to which the maps apply. Blue circles and red squares denote the 21 Hz and 26–29 Hz group of trials, respectively. The two sets of computed MDS maps clearly show a progressive separation of the two sets of trial frequencies as the trial evolves for all subjects. The early maps show some intermixing of the trials of 21 Hz and 26–29 Hz than do the maps some milliseconds later. In the later maps the two colors are drawn apart further and are more organized, with a better structure to the arms of the spanning tree and with the colors falling farther apart. Detailed examination of the maps show that for subjects 1 and 4 where the second map is taken earlier than that for subjects 2 and 3 the second maps are clearly less well organized. This supports the hypothesis that frequency discrimination is an early function of the left-SI area and that this process continues as time progresses. Further support comes from the later rise to significance for the all 21 Hz RQ analysis (Fig. 4) compared with the 21 Hz against 26–29 Hz results (Fig. 5). The mean time to significance is approximately 190 ms (±150 ms) for the former and approximately 70 ms (±20 ms) for the latter. To investigate whether the clusters derived from two time intervals as shown in the middle and right columns of Fig. 5 are the same or not topographically, we projected the clusters from the later latency range (right column) onto the reduced space defined by the clusters from the early latency range (middle column) using an “appending technique” (Laskaris and Ioannides, 2002). The superimposition of all four clusters onto the same reduced MDS map showed that the clustering at the later latency range is different from that at the early latency range.

We now test for correlates of perception and decision in the left-SI activation, which, if present, are expected toward the end of the Stim2 period. In the analysis of Fig. 5, we used both correct and incorrect response trials. If any part of the left-SI response has a perceptual or decision related influence, then the difference between the correct responses only should be higher than that between the entire two sets of trials in Fig. 5. We therefore selected two

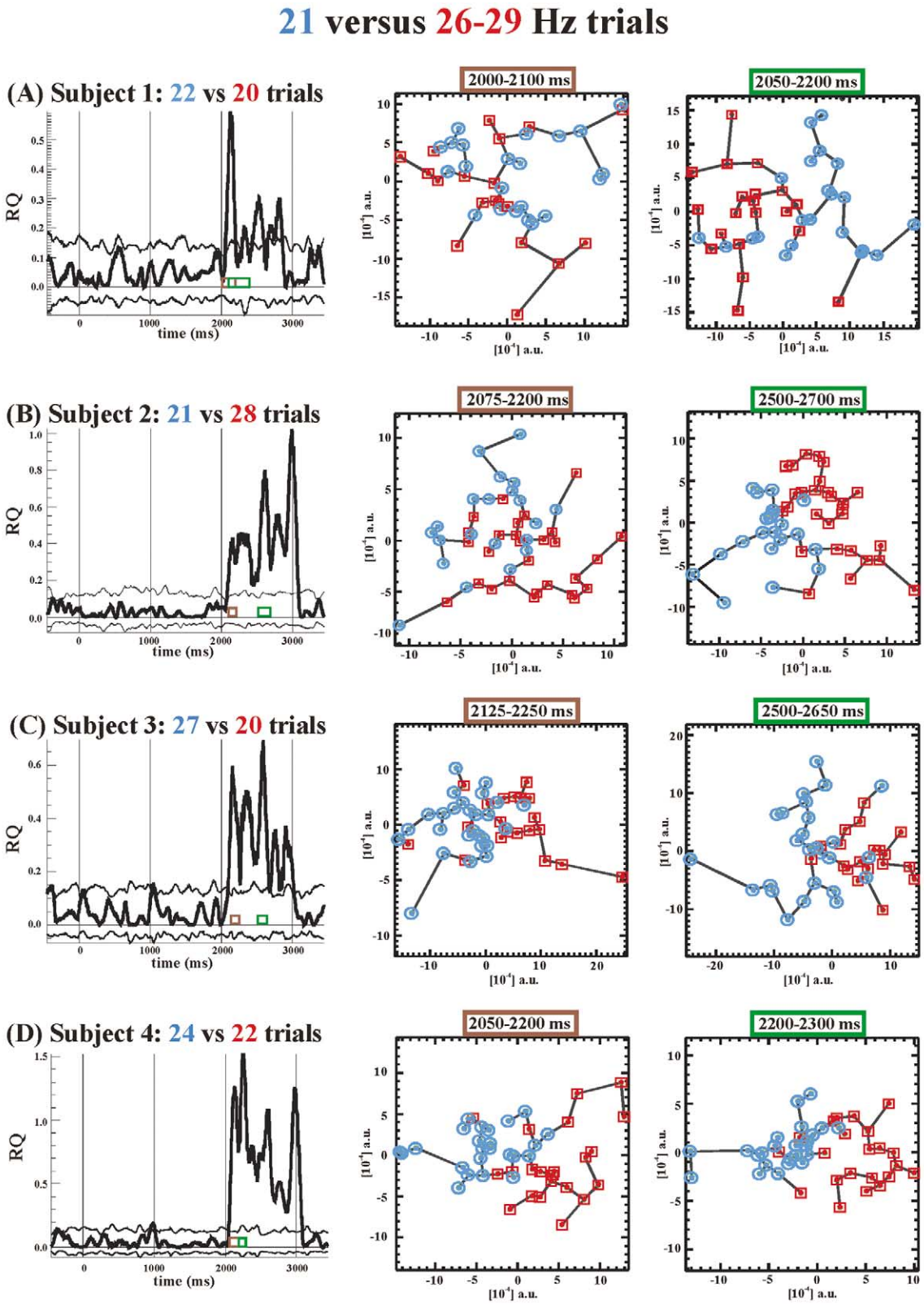

Fig. 5. Subjects 1–4 (A–D): comparison between trials of Stim2 at 21 Hz and 26–29 Hz. Left column: RQ(t) curve (thick black line) and its marker of significant level $P<0.05$ (two thin lines). The two early significant peaks of the RQ(t) curve were marked with a brown and green bar, respectively. Middle and right columns: MDS maps corresponding to the time ranges around the two early peaks of the RQ(t). Blue circles and red squares denote the trials of Stim2 at 21 Hz and 26–29 Hz trials, respectively.

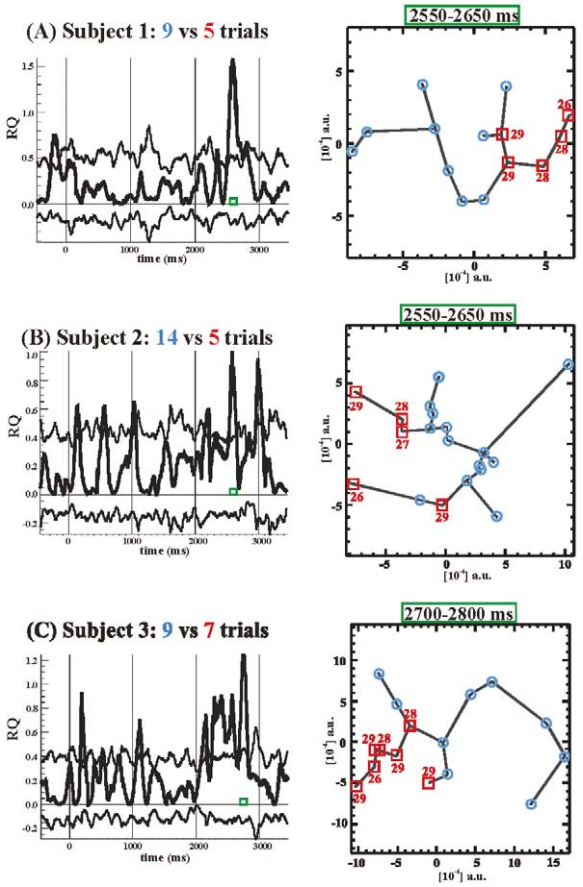

Fig. 6. Subjects 1–3 (A–C): comparison between correct 21 Hz and correct 26–29 Hz responses using the same annotation as in Fig. 5. On the MDS maps the true frequencies of Stim2 is printed in red text for the 26–29 Hz (red) nodes.

subsets of trials corresponding to the correct responses only in Fig. 5 and computed the RQ(t) for the comparison between correct 21 Hz and correct 26–29 Hz (i.e. response was the same as the input frequency of Stim2). We predicted that a high RQ would be found toward the end of the Stim2 period. In this comparison for all subjects there are only few trials in the 26–29 Hz correct responses but the analysis is unlikely to be affected, as both RQ and MDS are independent of the number of trials (Eq. 1). Subject 4 had only one correct response for the higher frequencies (26–29 Hz) and so was excluded from the following figure.

The results are shown in Fig. 6, the number of trials is given above the RQ(t) values in the left column, while the right column is the MDS plots with their times of analysis above. These times are shown as a green bar under the RQ(t) curves. In comparison with the results in Fig. 5, the results in Fig. 6 show a higher RQ(t) value (approximately 1.3–3 times higher) in the second part of the Stim2 trial and at that time (maximum significance of the RQ(t) peak) the MDS maps show a very clear separation of the two frequency sets. This result suggests that the latter part of the Stim2 epoch after separation of the groups may be related to the perception and decision of the subject.

Subject 4 was excluded from the above analysis because of very few absolutely correct trials suggesting that he was not able to discriminate between the high frequencies; he was however able to perform the comparison between 21 Hz and 22–29 Hz. Fig. 7A shows the result of RQ(t) and MDS analysis obtained from the correct 21 Hz against correct 22–29 Hz (although the trials are mainly 22 Hz) and it shows the RQ(t) with a MDS map taken from the area of the highest RQ peak marked by the green bar. The results show that the subject was able to distinguish between 21 Hz and 22–29 Hz successfully as both the RQ(t) and the MDS maps shows a very clear separation of the different groups of trials with the pattern of RQ(t) and MDS maps being similar to Fig. 6.

For subject 4 (but not for the other three subjects) there were enough examples for contrasting trials of 21 Hz response 21 Hz, against 26–29 Hz response 21 Hz (different input but same response). Toward the end of Stim2 if perception influences the left-SI activation then this contrast should show as a relative reduction of the RQ(t) coefficient. If that analysis is compared with the contrast of 21 Hz response 21 Hz, against 26–29 Hz response NOT 21 Hz (different input and different response) then toward the end of Stim2, when the influence of perception and decision occurs the RQ(t) should be higher than the earlier contrast. A difference at the end of the Stim2 trial would be added evidence for a perceptual and decision activity in the left-SI. Fig. 7B and 7C give the results for the above two comparisons, respectively. Fig. 7B is the RQ analysis of 21 Hz correct against 26–29 Hz (response 21 Hz) and shows a high RQ at the beginning of Stim2 as would be expected (Fig. 5) during the processing phase. Toward the end of the Stim2 epoch at approximately 650 ms the difference between the two groups reduces, the RQ value falls and intermittently becomes non-significant. This similarity between the two groups is concordant with the *perception* of both groups as 21 Hz. Fig. 7C is the analysis of the 21 correct against 22–29 Hz (response NOT 21 Hz) and again shows a high RQ at the beginning of Stim2 during the processing phase. Toward the end of the Stim2 the difference between the two groups again reduces, the RQ(t) value falls but never becomes non-significant. It does however rise again sharply at the end of the epoch to its highest value. The difference in the two groups is thus maintained throughout Stim2 and the raised RQ(t) in the last part of the epoch also is concordant with the perception that Stim1 and Stim2 remain different, e.g. NOT 21 Hz.

This effect can be further clarified using MDS maps. The maps should show a progressive differentiation of the three groups, 21 Hz response 21 Hz, 26–29 Hz response 21 Hz and 26–29 Hz response NOT 21 Hz. This analysis can only be done for this subject as there were a sufficient number of trials for these three groups. The analysis is shown at the bottom of Fig. 7. In Fig. 7D the map calculated early in Stim2 (2050–2250 ms) shows the 21 Hz, response 21 Hz (blue), as forming one cluster with the 26–29 Hz, response 21 (green) and 26–29 Hz, response NOT 21 Hz (red), forming another. Shown in Fig. 7E is the map calculated at the end of the Stim2 period (2800–3000

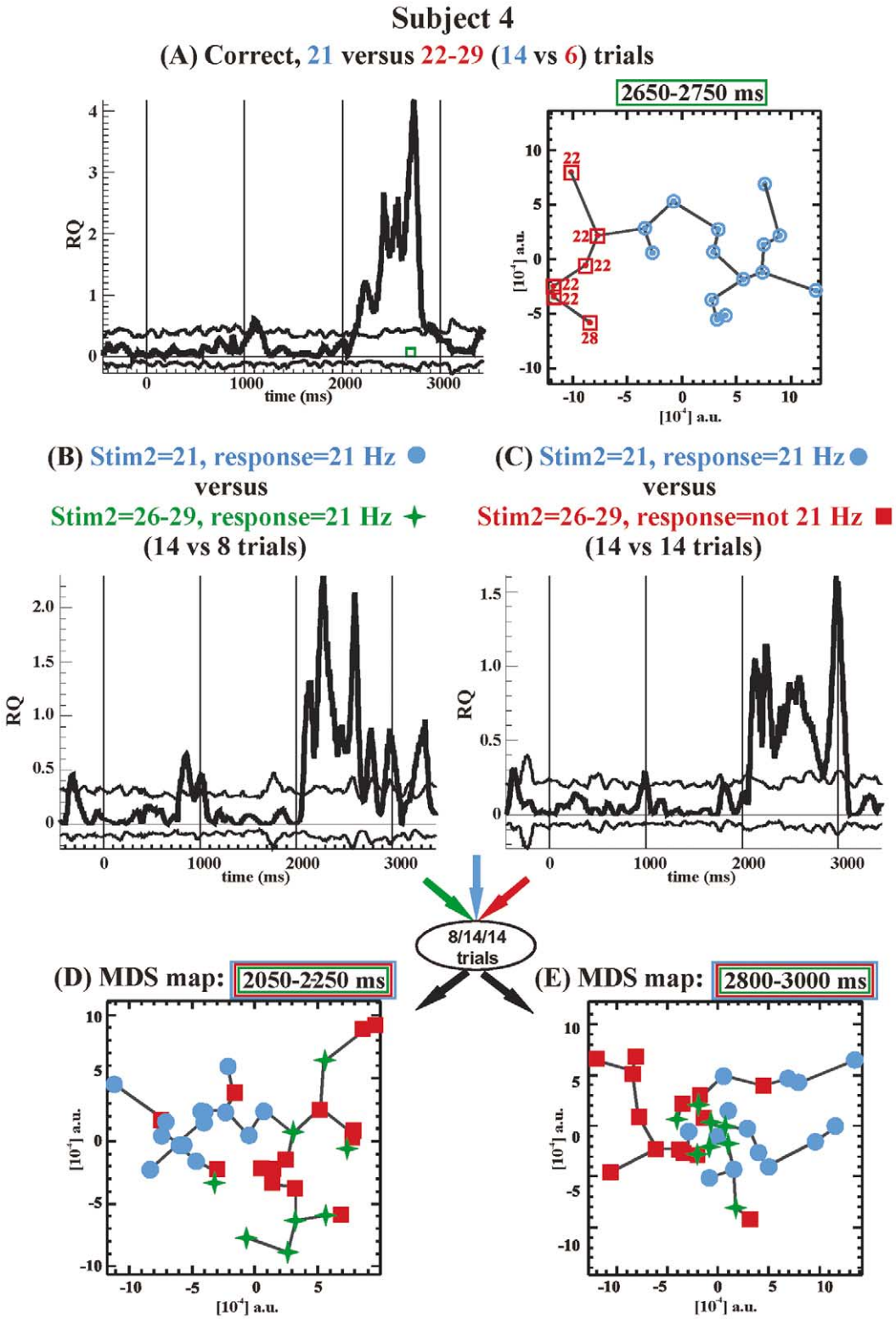

Fig. 7. Subject 4. (A) RQ and MDS analysis for the two groups of trials: correct 21 Hz and correct 22–29 Hz. (B) RQ(t) analysis for two groups of trials with different input frequency but same response (Stim2=21 Hz, response=21 Hz versus Stim2=26–29 Hz, response=21 Hz). (C) RQ(t) analysis for two groups of trials with different input frequency and different response (Stim2=21 Hz, response=21 Hz versus Stim2=26–29 Hz, response not 21 Hz). (D) The MDS map shows the above three contrasts, input 21 Hz, response 21 Hz (blue), input 26–29 Hz, response 21 Hz (green), input 26–29 Hz response not 21 Hz, (red) calculated over 2050–2250 ms near the beginning of the Stim2 epoch. (E) The MDS map with the same groups as in (D) calculated over 2800–3000 ms at the end of the Stim2 epoch.

ms), the three groups are now more separated. The 26–29 Hz, response 21 Hz (green), coming to lie closer to the perceptual group with which it has been misclassified by the subject, 21 Hz, response 21 Hz (blue), and it also lies between the other two groups. The trials with 26–29 Hz input and response NOT 21 Hz (red) now forms a more distinct group on their own, being differentiated from the other two groups. This suggests that the subjects' perception/decision is concordant with late Stim2 SI activity.

If the suggestion that surrounding the time of the highest RQ peak the analysis culminates in left-SI decision-making then an examination of the acv-curves from the period most successfully separated by the MDS maps should give an insight into the morphology of the acv-curves and the mechanisms underlying their generations. The results of this analysis are shown in Fig. 8.

The data from the correct 21 Hz versus the correct 26–29 Hz analysis in Fig. 6 were used. The chosen acv-curves were those three with the specific patterns defined as the ones with two-dimensional images on the two branches of the MST most distant away from the central limb and each other in the MDS map. The actual acv-curves chosen are shown as filled symbols (blue 21 Hz and red 26–29 Hz with their frequency beside them) in Fig. 8. For each subject the acv-curves are shown from 200 ms before to 200 ms after the 100 ms window used in the MDS map in Fig. 6. The time window of the MDS is shown over the MDS figure for each subject. Subject 4 was also included but as he had so few correct responses above 26 Hz, the frequency range reflecting the input for the RQ(t) and MDS analysis was increased to 22–29 Hz. The results are shown in three rows, the top two rows, 26–29 Hz (red) for subjects 1–3 or 22–29 Hz (red) for subject 4 and 21 Hz (blue). The third row is the average curves for the above two sets. It can be seen that for the 21 Hz there is clear phase reordering resulting in phase coherence across single trial acv-curves for the analysis period. This is less clear for the high frequencies but is still present. Amplitude enhancement is seen best for the 21 Hz while some attenuation is seen for the high frequencies. The phase re-organization and the amplitude modulation in the left-SI activity would seem to be present at the time the activity moves from analysis to decision.

DISCUSSION

Using our single trial tomographic analysis (MFT) of the MEG signal, we were able to track the path of any signal across the entire brain millisecond by millisecond. We found the most consistent focally activated area was over the left-SI in the hand region following electrical stimulation of the right-hand digits 2+3+4. After the onset of Stim1, the first activation peak was seen in the left-SI between 35 ms and 48 ms for all four subjects. Both the spatial and temporal profile of the activated area in SI were in agreement with recent neuroimaging studies using similar electrical (Kurth et al., 1998; Pollok et al., 2002; Forss et al., 2001) or mechanical stimuli (Gelnar et al., 1998; Tobimatsu et al., 1999; Iguchi et al., 2001) applied to human finger(s). The major difference between our work and the above MEG/EEG studies is that we used tomographic and pattern analysis of single trial MEG data, correlated with subjects' perception of the input frequency. Evidence for localization accuracy using the same tomographic analysis is shown in our two most recent works. The first work deals explicitly with the separation between SI and SII activations in single trials following simple, passive electrical stimulation (Ioannides et al., 2002). In this paper, we showed clearly that we could identify and separate the activation from SI and SII, and that different modes, i.e. featuring serial or parallel processing are encountered in different single trials following identical electrical median nerve stimulation. The second work demonstrated that the mean separation between V1 activation centers identified by fMRI and the earliest MEG activation at approximately 40 ms was 3–5 mm (Moradi et al., 2003). This result provides indirect, but strong evidence for the localization of SI and SII individually and the ability to separate their activations. The SI area is easier to identify with MEG than the corresponding V1 because the left and right representations of the body are further apart for upper limbs and it is easier to ensure that the stimulus is presented at the correct "spot" on the periphery while in vision one has always to worry about small eye movements.

Having validated our source reconstruction, we quantified the signal content in the single trial acv-curves for the left-SI ROI using the SNR measurements. As shown in Fig. 3, the single trial acv-curve activations had high SNR values and reflected the temporal resonance of the input frequency at 21 Hz and at the other frequencies (this was also observed in the wide-band acv-curves; not shown), confirming the findings reported in previous studies using similar steady-state stimuli (Tobimatsu et al., 1999; Liu et al., 2000).

We then proceeded to study the role of left-SI in the frequency discrimination task. Monkey studies using a discrimination task between the frequencies of two flutter stimuli (10–40 Hz) presented sequentially on a finger tip have shown that the firing rates of more than 50% of the sampled neurons (188 of 223 recorded) were significantly modulated by stimulus frequency (Hernandez et al., 1997, 2000; Salinas et al., 2000). Furthermore, neuronal and behavioral responses co-varied in single trials. Thus, the monkey studies showed that sensory activity provided input to memory and decision-making mechanisms (Romo and Salinas, 2001). The present study analyzed the subjects' behavioral and brain response using single trial acv-curve analysis. The methods we employed for this analysis were essentially similar to those used by Nicolelis et al. (1998), who used simultaneous multi-site neural ensemble recordings to investigate the representation of tactile location information in somatosensory areas (3b, SII and 2) and showed that neurons in these areas were able to identify correctly the location of a single tactile stimulus on a single trial within the first 45 ms. In our work, we used the RQ index to test putative encoding schemes. The RQ analysis was not significantly limited by the few trials available in some of the groups. We then used the MDS anal-

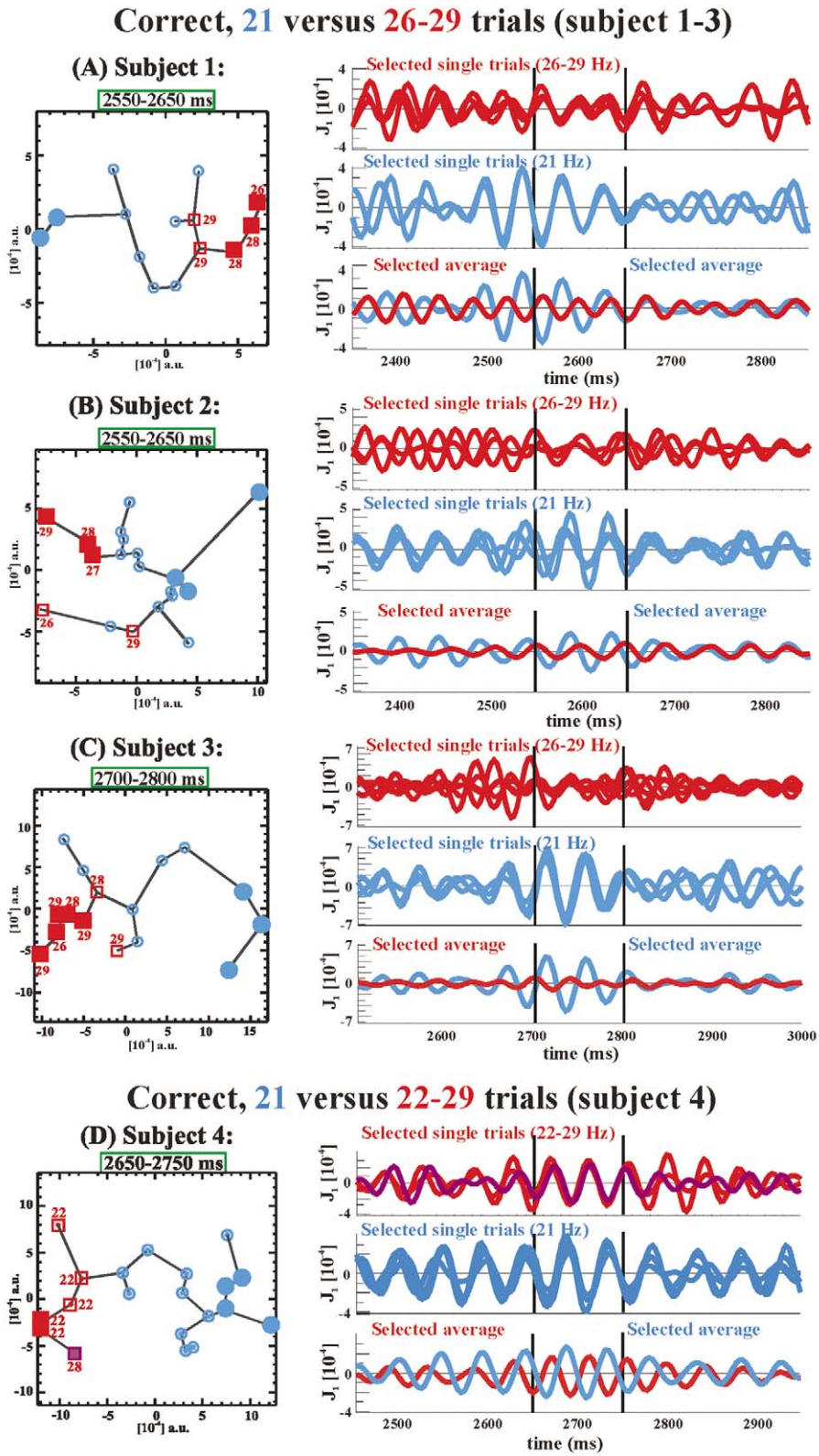

Fig. 8. Subjects 1–4 (A–D): MDS-based exploratory analysis of the correct responses in the MDS plot of Fig. 6. Two subsets of acv-curves were delineated. The images of these curves formed well-isolated branches in the overall MST, as shown in the left column. The single trial acv-curves for the 26–29 Hz (A–C) or the 22–29 Hz (D) (top red curves) and the 21 Hz (middle blue curves) group and the corresponding sub-averages for the two groups (bottom curves) are shown in the right column for a time range 200 ms before to 200 ms after the latency range for which the MDS plots were obtained. For each subject, this latency range is printed on the left column and also marked by the short thick vertical lines on the right column of the figure.

ysis to study the interactions between input frequency and the subject's perception and response. When we superimpose the clusters derived from two latency ranges onto the same reduced space, we found that the clustering at the two latency ranges was different suggesting that they are generated by different neuronal mechanisms.

With the millisecond temporal resolution provided by the MEG recording, we were able to explore the role of SI at different latencies and found that the left-SI activation reflected the input frequencies of Stim2 at early latencies (during the first 600 ms) but correlated with perception of the input frequency at later latencies (between 650 and 1000 ms). The higher RQ values at later latencies (Fig. 6 versus Fig. 5) suggests that the left-SI neural response is influenced by both the input frequencies of (Stim1 and Stim2) and reflects the perceived frequency and hence the verbal response. Although there was variability within single trials for the same subject and across subjects due to different strategy used for the discrimination, as indicated by the subjects during the interviews after the experiment, we introduced a type of analysis that could identify commonalities across all four subjects in the presence of variability. The subjects belonged to the same general group in terms of being normal right-handed males. It is likely that the commonalities in the role of SI we have identified in all four subjects reflect the role of SI among a general subject pool.

Using MEG to record the brain activity non-invasively, we have shown that the human SI response is likely to contain components related to stimulus frequency and subject perception, and hence in this respect is similar to the SI responses reported in monkeys (Romo and Salinas, 2001). Fig. 8 shows that the SI analysis and perception results are encoded in the single trial acv-curve by either phase reordering, phase coherence and/or low amplitude changes. A study of the morphology of acv-curves and their information content has shown that information is held in different ways (Laskaris and Ioannides, 2002). Phase reordering, phase shifting, frequency changing and amplitude alteration are all involved. Our data show some of these mechanisms in the SI activity.

A question relates to the experimental design which has two stimulation periods Stim1 and Stim2. The comparison between Stim1 and Stim2 with all the 21 Hz trials (Fig. 4) shows that after an initial common processing around 100 ms the RQ(t) begins to increase suggesting a different function for the Stim2 period. A further question relates to perception and decision and whether the conclusion is justified that this occurs in the later segment of the Stim2 trial. The data in Fig. 5 show a progressive separation of the two input frequencies as the Stim2 epoch progresses. If the analysis of the signal is taking place in left-SI then it is unlikely that a decision could be made before the frequencies had been analyzed. This leaves the later part of the epoch for decision, when, as Fig. 6 shows, the MDS maps are separate. Fig. 7 shows that subject 4 does show an RQ difference at the end of the Stim2 epoch as predicted when the decision only is different in the analysis, correct 21 Hz as against NOT 21 Hz. Although we have shown a relationship of left-SI with the decision it does not mean that the decision was made there. An analogous case is proposed for the MT neurons in the monkey (Newsome, 1997) that reflect aspects of eye movement decision in their late activations of moving stimuli. This is similar in our study to the modulation of SI activity related to the decision process.

There is an apparent delay in latency between the SI response reflecting the analysis of the input frequency and the output of decision-making operations. These findings generate new questions. Does SI activity continue between these two stages, when presumably further processing takes place in other areas? What other brain areas may work together with SI as the decision is made in the perceptual tasks of frequency discrimination? Candidate areas to explore would be secondary somatosensory cortex (SII), the prefrontal and the medial premotor cortex (MPC). These three areas belong to the ventral somatosensory stream that is likely to be associated with fine discrimination and recognition of stimulus patterns. SII is strongly connected to SI (Burton et al., 1995; Krubitzer et al., 1995), and information is processed mostly serially from SI to SII (Pons et al., 1987, 1992; Ioannides et al., 2002). Monkey studies by the Romo group have shown significant stimulus-driven modulations in firing rate in SII, and that the single trial covariations between behavioral and neuronal responses were much more evident in SII than in SI (Salinas et al., 2000; Romo et al., 2002). During the delay period between the two stimuli, neurons in the inferior convexity of the prefrontal cortex fired as a monotonic function of the first stimulus frequency (Romo et al., 1999). In comparison, neurons in MPC responded in correlation with the diverse stages of the discrimination process (Hernandez et al., 2002). Another candidate brain area for involvement in the decision making process is the thalamus. Ghazanfar et al. (2000) investigated how neurons in SI and the ventral posterior medial (VPM) nucleus of the thalamus of the anesthetized rat on a single trial basis may encode the location of a single whisker stimulus, and suggested that the representation of somatosensory features in the rat trigeminal system may arise from the interactions of neurons within and between the SI cortex and VPM nucleus. In another study using awake and free moving rats, Fanselow et al. (2001) showed that during the whisker twitching behavior, a descending signal from SI triggered thalamic bursting that primed the thalamocortical loop for enhanced signal detection.

In conclusion, we found neuronal activity of SI driven initially by the stimulus properties but reflecting later the perception of stimulus frequency. This paper has focused exclusively on the SI responses, as the first necessary step in tracing the wider network that must be involved in the perceptual decision process. Some of the candidate areas mentioned above are likely to produce as good an MEG signal as SI in single trials, but their activity will be less time-locked and hence difficult to pick up from the average of a few trials. Our identification of SI responses in single trials provides the thread to guide us to the other areas, in fairly direct, albeit computationally demanding ways.

REFERENCES

Braun C, Wilms A, Schweizer R, Godde B, Preissl H, Birbaumer N (2000) Activity patterns of human somatosensory cortex adapt dynamically to stimulus properties. Neuroreport 11:2977–2980.

Barrie JM, Holcman D, Freeman WJ (1999) Statistical evaluation of clusters derived by nonlinear mapping of EEG spatial patterns. J Neurosci Methods 90:87–95.

Burton H, Fabri M, Alloway K (1995) Cortical areas within the lateral sulcus connected to cutaneous representations in areas 3b and 1: a revisited interpretation of the second somatosensory area in macaque monkeys. J Comp Neurol 355:539–562.

Cohen A (1986) Biomedical signal processing. Vol. II. Compression and automatic recognition. CRC Press.

Fanselow EE, Sameshima K, Baccala LA, Nicolelis MA (2001) Thalamic bursting in rats during different awake behavioral states. Proc Natl Acad Sci USA 98:15330–15335.

Forss N, Narici L, Hari R (2001) Sustained activation of the human SII cortices by stimulus trains. Neuroimage 13:497–501.

Gelnar PA, Krauss BR, Szeverenyi NM, Apkarian AV (1998) Fingertip representation in the human somatosensory cortex: an fMRI study. Neuroimage 7:261–283.

Ghazanfar AA, Stambaugh CR, Nicolelis MA (2000) Encoding of tactile stimulus location by somatosensory thalamocortical ensembles. J Neurosci 20:3761–3775.

Hernandez A, Salinas E, Garcia R, Romo R (1997) Discrimination in the sense of flutter: new psychophysical measurements in monkeys. J Neurosci 17:6391–6400.

Hernandez A, Zainos A, Romo R (2000) Neuronal correlates of sensory discrimination in the somatosensory cortex. Proc Natl Acad Sci USA 97:6191–6196.

Hernandez A, Zainos A, Romo R (2002) Temporal evolution of a decision-making process in medial premotor cortex. Neuron 33: 959–972.

Iguchi Y, Hoshi Y, Hashimoto I (2001) Selective spatial attention induces short-term plasticity in human somatosensory cortex. Neuroreport 12:3133–3136.

Ioannides AA, Bolton JPR, Clarke CJS (1990) Continuous probabilistic solutions to the biomagnetic inverse problem. Inverse Problem 6:523–542.

Ioannides AA, Kostopoulos G, Laskaris N, Liu LC, Shibata T, Schellens M, Poghosyan V, Khurshudyan A (2002) Timing and connectivity in the human somatosensory cortex from single trial mass electrical activity. Hum Brain Mapp 15:231–246.

Jahn O, Cichocki A, Ioannides AA, Amari S (1999) Identification and elimination of artifacts from MEG signals using extended independent component analysis. In: Recent advances in biomagnetism (Yoshimoto T, Kotani M, Kuriki S, Karibe H, Nakasato N, eds), pp 224–228. Sendai: Tohoku University Press.

Jain A, Dubes R (1988) Algorithms for clustering data, pp 55–141. New Jersey: Prentice Hall.

Kurth R, Villringer K, Mackert BM, Schwiemann J, Braun J, Curio G, Villringer A, Wolf KJ (1998) fMRI assessment of somatotopy in human Brodmann area 3b by electrical finger stimulation. Neuroreport 9:207–212.

Krubitzer L, Clarey J, Tweendale R, Elston G, Calford MA (1995) A redefinition of somatosensory areas in the lateral sulcus of macaque monkeys. J Neurosci 15:3821–3839.

Laskaris N, Fotopoulos S, Papathanasopoulos P, Bezerianos A (1997) Robust moving averages, with Hopfield neural network implementation, for the monitoring of evoked potential signals. Electroenceph Clin Neurophysiol 104:151–156.

Laskaris N, Ioannides AA (2001) Exploratory data analysis of evoked response single trials based on minimal spanning tree. Clin Neurophysiol 112:698–712.

Laskaris N, Ioannides AA (2002) Semantic geodesic maps: a unifying geometrical approach for studying the structure and dynamics of single trial evoked responses. Clin Neurophysiol 113:1209–1226.

Liu LC, Gaetz WC, Bosnyak DJ, Roberts LE (2000) Evidence for fusion and segregation induced by 21 Hz multiple-digit stimulation in humans. Neuroreport 11:2313–2318.

Miller EK, Cohen JD (2001) An integrative theory of prefrontal cortex function. Annu Rev Neurosci 24:167–202.

Moradi F, Liu LC, Cheng K, Tanaka K, Ioannides AA (2003) Consistent and precise localization of brain activity in human primary visual cortex by MEG and fMRI. NeuroImage 18:595–609.

Newsome WT (1997) The King Solomon lectures in neuroethology: deciding about motion: linking perception to action. J Comp Physiol [A] 181:5–12.

Nicolelis MAL, Ghazanfar AA, Stambaugh CR, Oliveira LMO, Laubach M, Chapin JK, Nelson RJ, Kaas JH (1998) Simultaneous encoding of tactile information by three primate cortical areas. Nat Neurosci 1:621–630.

Pollok B, Moll M, Schmitz F, Muller K, Schnitzler A (2002) Rapid mapping of finger representations in human primary somatosensory cortex applying neuromagnetic steady-state responses. Neuroreport 13:235–238.

Pons TP, Garraghty PE, Friedman DP, Mishkin M (1987) Physiological evidence for serial processing in somatosensory cortex. Science 237:417–420.

Pons TP, Garraghty PE, Mishkin M (1992) Serial and parallel processing of tactual information in somatosensory cortex of rhesus monkeys. J Neurophysiol 68:518–527.

Raz J, Turetsky B, Fein G (1988) Confidence intervals for signal-to-noise ratio when a signal embedded in noise is observed over repeated trials. IEEE Trans Biomed Eng 8:646–649.

Recanzone GH, Jenkins WM, Hradek GT, Merzenich MM (1992) Progressive improvement in discriminative abilities in adult owl monkeys performing a tactile frequency discrimination task. J Neurophysiol 67:1015–1030.

Romo R, Hernandez A, Zainos A, Salinas E (1998) Somatosensory discrimination based on cortical microstimulation. Nature 392:387–390.

Romo R, Brody CD, Hernandez A, Lemus L (1999) Neuronal correlates of parametric working memory in the prefrontal cortex. Nature 399:470–473.

Romo R, Hernandez A, Zainos A, Brody CD, Lemus L (2000) Sensing without touching: psychophysical performance based on cortical microstimulation. Neuron 26:273–278.

Romo R, Salinas E (2001) Touch and go: decision-making mechanisms in somatosensation. Annu Rev Neurosci 24:107–137.

Romo R, Hernandez A, Zainos A, Lemus L, Brody CD (2002) Neuronal correlates of decision-making in secondary somatosensory cortex. Nat Neurosci 5:1217–1225.

Salinas E, Hernandez A, Zainos A, Romo R (2000) Periodicity and firing rate as candidate neural codes for the frequency of vibrotactile stimuli. J Neurosci 20:5503–5515.

Schall JD (2001) Neural basis of deciding, choosing and acting. Nat Rev Neurosci 2:33–42.

Tobimatsu S, Zhang YM, Kato M (1999) Steady-state vibration somatosensory evoked potentials: physiological characteristics and tuning function. Clin Neurophysiol 110:1953–1958.

(Accepted 23 April 2003)